Matching-pursuit/split-operator-Fourier-transform computations of thermal correlation functions

Xin Chen, Yinghua Wu, and Victor S. Batista
Department of Chemistry, Yale University, New Haven, Connecticut 06520-8107

(Received 12 October 2004; accepted 19 November 2004; published online 1 February 2005)

A rigorous and practical methodology for evaluating thermal-equilibrium density matrices, finite-temperature time-dependent expectation values, and time-correlation functions is described. The method involves an extension of the matching-pursuit/split-operator-Fourier-transform method to the solution of the Bloch equation via imaginary-time propagation of the density matrix and the evaluation of Heisenberg time-evolution operators through real-time propagation in dynamically adaptive coherent-state representations. © *2005 American Institute of Physics*.
[DOI: 10.1063/1.1848513]

I. INTRODUCTION

Rigorous and practical quantum-mechanical methods for computations of equilibrium and dynamical properties of complex systems (e.g., systems with many degrees of freedom) have yet to be established. This paper introduces one such method as an extension of the recently developed matching-pursuit/split-operator-Fourier-transform (MP/SOFT) method[1–3] to calculations of thermal-equilibrium averages and finite-temperature time-dependent expectation values and time-correlation functions.

In recent years, there has been significant progress in the development of numerically exact methods[4–16] for quantum dynamics propagation based on the SOFT approach,[17–19] the Chebyshev expansion,[20] or the short iterative Lanczos[21] algorithms. These rigorous approaches, however, are limited to systems with very few degrees of freedom (e.g., molecular systems with less than three or four atoms) since they require storage space and computation effort that scale exponentially with the number of coupled degrees of freedom. Such an exponential scaling problem has limited studies of thermal correlation functions of complex systems to approximate methods built around semiclassical approximations,[22–24] mixed quantum-classical treatments,[25,26] centroid molecular dynamics,[27–29] analytic-continuation of imaginary-time path-integral Monte Carlo data,[30,31] or the self-consistent mode-coupling theory.[32,33] However practical, these approximate approaches require a compromise between accuracy and feasibility and rely on *ad hoc* approximations whose resulting consequences are often difficult to quantify in applications to complex (nonintegrable) dynamics. It is, therefore, essential to develop practical methods for rigorous computations of time-correlation functions of complex systems. Such methods would allow one to validate approximate approaches and provide new insights into the nature of quantum processes.

The MP/SOFT method[1–3] has been recently introduced in an effort to develop a simple and rigorous time-dependent method for simulations of quantum processes in multidimensional systems. The MP/SOFT methodology is based on the recursive application of the time-evolution operator, as defined by the Trotter expansion to second-order accuracy, in nonorthogonal and dynamically adaptive coherent-state representations generated according to the matching-pursuit algorithm.[34] The main advantage of this approach relative to the standard grid-based SOFT method is that the coherent-state expansions allow for an *analytic* implementation of the Trotter expansion, bypassing the exponential scaling problem associated with the fast-Fourier-transform algorithm of usual grid-based implementations. When compared to other time-dependent methods based on coherent-state expansions,[35–49] the MP/SOFT method has the advantage of avoiding the usual need of propagating expansion coefficients by solving a coupled system of differential equations. Further, the MP/SOFT method implements a successive orthogonal decomposition scheme that overcomes the usual numerical difficulties due to overcompleteness introduced by nonorthogonal basis functions.[8] The main drawback of the MP/SOFT method is that it requires generating a new coherent-state expansion of the time evolving state for each propagation step, although the underlying computational task can be trivially parallelized.

The capabilities of the MP/SOFT method for simulations of quantum dynamics in multidimensional systems have already been demonstrated as applied to simulations of tunneling dynamics in model systems with up to 35 coupled degrees of freedom.[2,50] There is, however, the nontrivial question as to whether such an approach can be efficiently implemented to provide accurate descriptions of thermal-equilibrium density matrices, finite-temperature time-dependent expectation values and time-correlation functions. This paper shows that the MP/SOFT methodology can indeed be effectively applied to computations of thermal correlation functions simply by combining the imaginary-time propagation of equilibrium density matrices with the evaluation of Heisenberg time-evolution operators via real-time propagation in dynamically adaptive coherent-state representations. While the paper is focused only on validating the MP/SOFT methodology by performing rigorous comparisons with benchmark calculations for reduced dimensional model systems, the results at least demonstrate the potentiality of

the MP/SOFT method as applied to the description of thermal correlation functions of complex (i.e., nonintegrable) quantum systems.

The paper is organized as follows. Section II describes the generalization of the MP/SOFT method to calculations of finite-temperature equilibrium density matrices by imaginary-time integration of the Bloch equation and the calculation of thermal correlation functions through evaluation of Heisenberg time-evolution operators via real-time propagation. Section III describes the implementation of the MP/SOFT method, as generalized in Sec. II, to the description of finite-temperature time-dependent expectation values and thermal correlation functions for a model system that allows for rigorous comparisons with benchmark calculations. Section IV summarizes and concludes.

II. METHODS

Consider the problem of computing thermal correlation functions,

$$C(t) = \langle A(0)B(t)\rangle = Z^{-1}\,\mathrm{Tr}[e^{-\beta\hat{H}_0}\hat{A}e^{i\hat{H}_1 t}\hat{B}e^{-i\hat{H}_1 t}], \tag{1}$$

where $\langle\cdots\rangle$ indicates the Boltzmann ensemble average at temperature $T=1/(k_B\beta)$, with k_B the Boltzmann constant; $\hat{A}$ and $\hat{B}$ are quantum-mechanical operators associated with measurements of observables at time 0 and t, respectively; $Z=\mathrm{Tr}[e^{-\beta\hat{H}_0}]$ is the canonical partition function; and $\hat{H}_j=-\nabla_{\mathbf{x}}^2/(2m)+V_j(\hat{\mathbf{x}})$ is the Hamiltonian of the system of interest with N degrees of freedom interacting according to the potential $V_j(\hat{\mathbf{x}})$. An example is the correlation function $C(t)$ for a system evolving on the excited state potential energy surface $V_1(\hat{\mathbf{x}})$, as would result from a photoexcitation process after the initial preparation at thermal equilibrium in the ground state potential energy surface $V_0(\hat{\mathbf{x}})$. To keep the notation as simple as possible, all expressions are written in mass-weighted coordinates and atomic units so that all degrees of freedom have the same mass m and $\hbar=1$.

Note that Eq. (1) provides an expression for computing not only time-dependent thermal correlation functions but also thermal-equilibrium ensemble averages $\langle A\rangle = Z^{-1}\,\mathrm{Tr}[e^{-\beta\hat{H}_0}\hat{A}]$, when $\hat{B}=1$, and finite-temperature time-dependent ensemble averages,

$$\langle B(t)\rangle = Z^{-1}\,\mathrm{Tr}[e^{-\beta\hat{H}_0}e^{i\hat{H}_1 t}\hat{B}e^{-i\hat{H}_1 t}], \tag{2}$$

when $\hat{A}=1$.

Thermal correlation functions $C(t)$ are obtained according to the following symmetrized form of Eq. (1):

$$C(t) = Z^{-1}\int d\mathbf{x}\int d\mathbf{x}'\int d\mathbf{x}''\langle\mathbf{x}|e^{-(\beta/2)\hat{H}_0}|\mathbf{x}'\rangle A(\mathbf{x}') \times\langle\mathbf{x}'|e^{i\hat{H}_1 t}\hat{B}e^{-i\hat{H}_1 t}|\mathbf{x}''\rangle\langle\mathbf{x}''|e^{-(\beta/2)\hat{H}_0}|\mathbf{x}\rangle. \tag{3}$$

The computational task necessary to obtain $C(t)$, according to Eq. (3), requires obtaining the matrix elements $A(\mathbf{x}')\times\langle\mathbf{x}'|e^{-(\beta/2)\hat{H}_0}|\mathbf{x}\rangle$ and $\langle\mathbf{x}''|e^{-(\beta/2)\hat{H}_0}|\mathbf{x}\rangle$ and the subsequent real-time propagation for time t, according to $\hat{H}_1$. The matrix elements are computed, as described below by imaginary-time integration of the Bloch equation according to $\hat{H}_0$. The extension of the MP/SOFT method, introduced in this paper, involves the numerically exact treatment of both the real- and imaginary-time propagation steps as described below for the imaginary-time propagation. The real-time propagation is analogously performed by simply implementing the variable transformation $\beta\rightarrow -it/\hbar$ from imaginary to real time.

The Boltzmann-operator matrix elements are obtained by solving the Bloch equation,[51]

$$\left\{\frac{\partial}{\partial\beta}-\frac{1}{2m}\nabla_{\mathbf{x}}^2+V_0(\mathbf{x})\right\}\rho(\mathbf{x},\mathbf{x}';\beta)=0, \tag{4}$$

for $\rho(\mathbf{x},\mathbf{x}';\beta)\equiv\langle\mathbf{x}|e^{-\beta\hat{H}_0}|\mathbf{x}'\rangle$ subject to the initial condition given by the high-temperature approximation,

$$\rho(\mathbf{x},\mathbf{x}';\epsilon)=\left(\frac{m}{2\pi\epsilon}\right)^{1/2}e^{-(\epsilon/2)[V_0(\mathbf{x})+V_0(\mathbf{x}')]}e^{-(m/2\epsilon)(\mathbf{x}-\mathbf{x}')^2}, \tag{5}$$

where ϵ defines a sufficiently high temperature $T=1/(k_B\epsilon)$.

Equation (4) is formally integrated as follows:

$$\rho(\mathbf{x},\mathbf{x}';\beta)=\int d\mathbf{x}''\rho(\mathbf{x},\mathbf{x}'';\beta-\epsilon)\rho(\mathbf{x}'',\mathbf{x}';\epsilon), \tag{6}$$

where the propagator $\rho(\mathbf{x},\mathbf{x}'';\beta-\epsilon)\equiv\langle\mathbf{x}|e^{-(\beta-\epsilon)\hat{H}_0}|\mathbf{x}''\rangle$ is imaginary time sliced by repeatedly inserting the resolution of identity,

$$\hat{\mathbf{1}}=\int d\mathbf{x}_j|\mathbf{x}_j\rangle\langle\mathbf{x}_j|, \tag{7}$$

yielding

$$\langle\mathbf{x}|e^{-(\beta-\epsilon)\hat{H}_0}|\mathbf{x}''\rangle=\int d\mathbf{x}_{s-1}\ldots\int d\mathbf{x}_1\langle\mathbf{x}|e^{-i\hat{H}_0\tau}|\mathbf{x}_{s-1}\rangle \times\ldots\langle\mathbf{x}_1|e^{-i\hat{H}_0\tau}|\mathbf{x}''\rangle, \tag{8}$$

where $\tau\equiv -i(\beta-\epsilon)/s$ is a sufficiently thin imaginary-time slice.

Each finite-time propagator, introduced by Eq. (8), is approximated for sufficiently small imaginary-time slices τ by the Trotter expansion to second-order accuracy,

$$e^{-i\hat{H}_0\tau}\approx e^{-iV_0(\hat{\mathbf{x}})\tau/2}e^{-i(\hat{\mathbf{p}}^2/2m)\tau}e^{-iV_0(\hat{\mathbf{x}})\tau/2}. \tag{9}$$

The MP/SOFT propagation of the initial condition, introduced by Eq. (5), according to the Trotter expansion introduced by Eq. (9) entails the following steps.

Step (1): Decompose $\tilde{\rho}(\mathbf{x},\mathbf{x}';\epsilon)\equiv e^{-iV_0(\mathbf{x})\tau/2}\rho(\mathbf{x},\mathbf{x}';\epsilon)$ in a matching-pursuit coherent-state expansion:

$$\tilde{\rho}(\mathbf{x},\mathbf{x}';\epsilon)\approx\sum_{j=1}^{n}c_j\phi_j(\mathbf{x})[\phi'_j(\mathbf{x}')]^*, \tag{10}$$

where $\phi_j(\mathbf{x})$ and $\phi'_j(\mathbf{x})$ are N-dimensional coherent states defined as follows:

$$\phi_j(\mathbf{x})\equiv\prod_{k=1}^{N}A_{\phi_j}(k)e^{-\gamma_{\phi_j}(k)[x(k)-x_{\phi_j}(k)]^2/2}e^{ip_{\phi_j}(k)[x(k)-x_{\phi_j}(k)]}, \tag{11}$$

with complex-valued coordinates $x_{\phi_j}(k)\equiv r_{\phi_j}(k)+id_{\phi_j}(k)$, momenta $p_{\phi_j}(k)\equiv g_{\phi_j}(k)+if_{\phi_j}(k)$ and scaling parameters

$\gamma_{\phi_j}(k) \equiv a_{\phi_j}(k) + ib_{\phi_j}(k)$. The normalization constants are $A_{\phi_j}(k) \equiv (a_{\phi_j}(k)/\pi)^{1/4} \exp\{-\frac{1}{2}a_{\phi_j}(k)d_{\phi_j}(k)^2 - d_{\phi_j}(k)g_{\phi_j}(k) - [b_{\phi_j}(k)d_{\phi_j}(k) + f_{\phi_j}(k)]^2/[2a_{\phi_j}(k)]\}$.

The expansion coefficients, introduced by Eq. (10), are defined as follows:

$$c_j \equiv \begin{cases} I_j, & \text{when } j = 1, \\ I_j - \sum_{k=1}^{j-1} c_k \langle \phi_j | \phi_k \rangle \langle \phi_k' | \phi_j' \rangle, & \text{for } j = 2 - n, \end{cases} \tag{12}$$

where the overlap integral I_j is defined as follows:

$$I_j \equiv \int d\mathbf{x}' d\mathbf{x} \phi_j(\mathbf{x}) \tilde{\rho}(\mathbf{x}, \mathbf{x}'; \epsilon) [\phi_j'(\mathbf{x}')]^* . \tag{13}$$

Step (2): Analytically Fourier transform the coherent-state expansion to the momentum representation, apply the kinetic energy part of the Trotter expansion, and analytically inverse Fourier transform the resulting expression back to the coordinate representation to obtain the imaginary-time evolved Boltzmann-operator matrix elements:

$$\rho(\mathbf{x}, \mathbf{x}'; \epsilon + i\tau) = \sum_{j=1}^{n} c_j e^{-iV_0(\mathbf{x})\tau/2} \tilde{\phi}_j(\mathbf{x}) [\phi_j'(\mathbf{x}')]^* , \tag{14}$$

where

$$\tilde{\phi}_j(\mathbf{x}) \equiv \prod_{k=1}^{N} A_{\tilde{\phi}_j}(k) \sqrt{\frac{m}{m + i\tau\gamma_{\tilde{\phi}_j}(k)}} \times \exp\left(\frac{\left(\frac{p_{\tilde{\phi}_j}(k)}{\gamma_{\tilde{\phi}_j}(k)} - i[x_{\tilde{\phi}_j}(k) - x(k)] \right)^2}{\left(\frac{2}{\gamma_{\tilde{\phi}_j}(k)} + \frac{i2\tau}{m} \right)} - \frac{p_{\tilde{\phi}_j}(k)^2}{2\gamma_{\tilde{\phi}_j}(k)} \right). \tag{15}$$

Note that the MP/SOFT approach reduces the computational task necessary for the imaginary- or real-time propagation of the Boltzmann-operator matrix elements $\rho(\mathbf{x}, \mathbf{x}'; \beta)$ to the problem of recursively generating the coherent-state expansions introduced by Eq. (10).

Coherent-state expansions are obtained by combining the matching-pursuit algorithm and a gradient-based optimization method as follows:

Step (1.1): Evolve the complex-valued parameters, that define the initial trial coherent states $\phi_j(\mathbf{x})$ and $\phi_j'(\mathbf{x})$, to locally maximize the overlap integral I_j, introduced in Eq. (13). The parameters $x_{\phi_1}(k), p_{\phi_1}(k), \gamma_{\phi_1}(k)$ and $x_{\phi_1'}(k), p_{\phi_1'}(k), \gamma_{\phi_1'}(k)$ of the corresponding local maximum define the first pair of coherent states ϕ_1 and ϕ_1' in the expansion introduced by Eq. (10) and the first expansion coefficient c_1 as follows: $\tilde{\rho}(\mathbf{x}, \mathbf{x}'; \epsilon) = c_1 \phi_1(\mathbf{x}) [\phi_1'(\mathbf{x}')]^* + \varepsilon_1(\mathbf{x}, \mathbf{x}')$, where $c_1 \equiv I_1$, as defined according to Eq. (13). The results reported in Sec. III were obtained by locally optimizing I_j according to a gradient-based optimization scheme that combines the steepest descent algorithm with the parabolic search approach.[52] Further, note that due to the definition of c_1, the residue $\varepsilon_1(\mathbf{x}, \mathbf{x}')$ does not overlap with the product state $\phi_1(\mathbf{x})[\phi_1'(\mathbf{x}')]^*$. Therefore, the norm of the remaining residue $\varepsilon_1(\mathbf{x}, \mathbf{x}')$ is smaller than the norm of the initial target state $\tilde{\rho}(\mathbf{x}, \mathbf{x}'; \epsilon)$, i.e., $\|\varepsilon_1\| < \|\tilde{\rho}\|$.

Step (1.2): Go to (1.1), replacing $\tilde{\rho}(\mathbf{x}, \mathbf{x}'; \epsilon)$ by $\varepsilon_1(\mathbf{x}, \mathbf{x}')$, i.e., subdecompose the residue by its projection along the direction of its locally optimum match as follows: $\varepsilon_1(\mathbf{x}, \mathbf{x}') = c_2 \phi_2(\mathbf{x}) [\phi_2'(\mathbf{x}')]^* + \varepsilon_2(\mathbf{x}, \mathbf{x}')$, where

$$c_2 \equiv \int d\mathbf{x}' \, d\mathbf{x} \phi_2(\mathbf{x}) \varepsilon_1(\mathbf{x}, \mathbf{x}') [\phi_2'(\mathbf{x}')]^* . \tag{16}$$

Note that $\|\varepsilon_2\| < \|\varepsilon_1\|$, since $\varepsilon_2(\mathbf{x}, \mathbf{x}')$ is orthogonal to the product state $\phi_2(\mathbf{x})[\phi_2'(\mathbf{x}')]^*$.

Step (1.2) is repeated each time on the resulting residue. After n successive projections, the norm of the residue ε_n is smaller than a desired precision ϵ, i.e., $\|\varepsilon_n\| = (1 - \sum_{j=1}^{n} |c_j|^2)^{1/2} < \epsilon$, and the resulting expansion is given by Eq. (10). Note that norm conservation of $\tilde{\rho}_\epsilon$ is maintained within a desired precision, just as in a linear orthogonal decomposition, although the coherent states in the expansion are nonorthogonal basis functions.

It is important to mention that the computational bottleneck of the MP/SOFT method involves the calculation of overlap matrix elements $\langle \phi_j | e^{-iV_j(\hat{\mathbf{x}})\tau/2} | \tilde{\phi}_k \rangle$ and $\langle \phi_j | e^{-iV_j(\hat{\mathbf{x}})\tau/2} | \phi_k \rangle$, where $|\phi_k\rangle$ and $|\tilde{\phi}_k\rangle$ are localized Gaussians introduced by Eqs. (11) and (15), respectively. The underlying computational task is however trivially parallelized according to a portable single-program-multiple-data streams code that runs under the message-passing-interface environment.

The overlap integrals are most efficiently computed in applications to reaction surface Hamiltonians where a large number of harmonic modes can be *arbitrarily* coupled to a few reaction (tunneling) coordinates (see, e.g., Models I and II in Ref. 3 and the reaction surface Hamiltonians in Refs. 53–55). For such systems, the Gaussian integrals over harmonic coordinates can be analytically computed and the remaining integrals over reaction coordinates are efficiently obtained according to numerical quadrature techniques. For more general Hamiltonians, the overlap matrix elements can be approximated by analytic Gaussian integrals when the choice of width parameters $\gamma_j(k)$ allows for a local expansion of $V_j(\hat{\mathbf{x}})$ to second-order accuracy. Otherwise, the quadratic approximation is useful for numerically computing the corresponding full-dimensional integrals according to variance-reduction Monte Carlo techniques.

III. RESULTS

The accuracy and efficiency of the MP/SOFT methodology, described in Sec. II, are evaluated in terms of explicit calculations of time-dependent position ensemble averages and position-position thermal correlation functions for the asymmetric quartic oscillator described by the following Hamiltonian:

$$\hat{H}_1 = \frac{\hat{p}^2}{2m} + V_1(x), \tag{17}$$

where

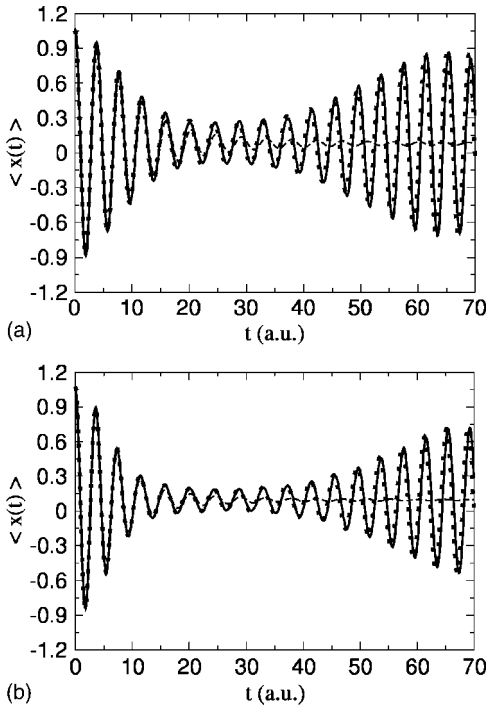

FIG. 1. Comparison of thermal ensemble average positions, obtained according to the MP/SOFT method (solid lines), benchmark grid-based SOFT calculations (dots), and classical ensemble averages (thin-dashed lines) for the asymmetric quartic potential introduced by Eq. (18). The system is initially prepared at thermal equilibrium on the potential energy surface introduced by Eq. (19) at two different temperatures corresponding to (a) $\hbar\omega\beta=\sqrt{2}$ and (b) $\hbar\omega\beta=\sqrt{2}/2$.

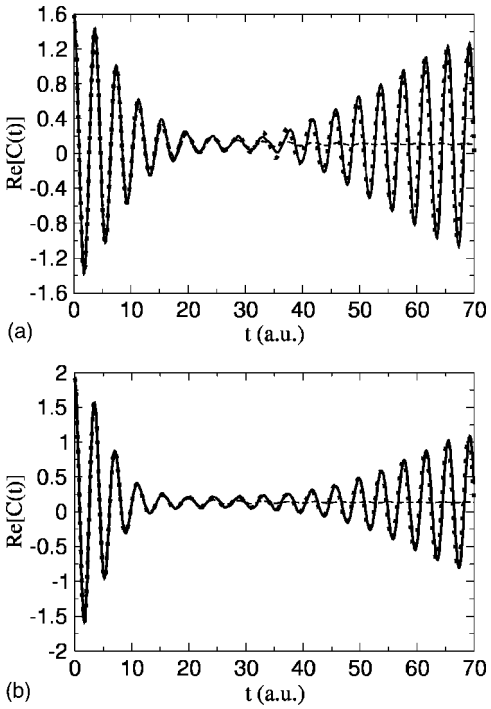

FIG. 2. Comparison of real parts of the position-position correlation functions obtained according to the MP/SOFT method (solid lines), benchmark grid-based SOFT calculations (dots), and the classical Boltzmann ensemble averages (thin-dashed lines) for the asymmetric quartic potential, introduced by Eq. (18). The system is initially prepared at thermal equilibrium on the potential energy surface introduced by Eq. (19) at two different temperatures corresponding to (a) $\hbar\omega\beta=\sqrt{2}$ and (b) $\hbar\omega\beta=\sqrt{2}/2$.

$$V_1(x) = \tfrac{1}{2}m\omega^2x^2 - cx^3 + cx^4, \tag{18}$$

with $m=1$ a.u., $\omega=\sqrt{2}$ a.u., and $c=0.1$ a.u. The system is initially prepared at thermal equilibrium on the displaced potential energy surface,

$$V_0(x) = \tfrac{1}{2}m\omega^2(x-a)^2 - c(x-a)^3 + c(x-a)^4, \tag{19}$$

with $a=1$ a.u.

The model system, introduced by Eqs. (17)–(19), is particularly interesting since the highly anharmonic potential leads to ultrafast dephasing within a few oscillation periods as well as later rephasing of wave packet motion due to the effect of quantum coherences. The underlying dynamics can be described by rigorous quantum-mechanical approaches and has been investigated in terms of semiclassical approaches based on coherent-state representations.[22,23,56] Therefore, the model is ideally suited for a rigorous analysis of the accuracy and efficiency of the MP/SOFT method as compared to classical, semiclassical, and benchmark quantum-mechanical calculations.

Figure 1 shows the time-dependent position ensemble averages $\langle\mathbf{x}(t)\rangle$, obtained according to the MP/SOFT methodology (solid lines) implemented according to Eq. (3), with $A(\mathbf{x}')=1$ and $\hat{B}=\hat{\mathbf{x}}$. The MP/SOFT results are compared to the corresponding benchmark grid-based SOFT calculations (dots) and the classical ensemble average predictions (thin-dashed lines) at two different temperatures, corresponding to $\hbar\omega\beta=\sqrt{2}$ and $\hbar\omega\beta=\sqrt{2}/2$, in panels (a) and (b), respectively. For reference, note that for a molecular vibration of $\omega=250$ cm^{-1} the two temperatures in panels (a) and (b) correspond to 254 K and 508 K, respectively.

The results shown in Fig. 1 indicate that during the early-time dynamics (i.e., within the first 20 a.u.) the relaxation of the system is dominated by classical dephasing due to the anharmonicity of the potential, a process that is faster at higher temperature. This early-time relaxation is therefore accurately described by classical mechanics, as indicated in Fig. 1 by the comparison between benchmark quantum-mechanical calculations (dots) and classical results (thin-dashed lines). Recurrencies at later times, however, are due to quantum-mechanical coherences and therefore require an accurate description of coherent wave packet motion. Consequently, classical results fail to describe recurrencies beyond $t\approx 20$ a.u. In contrast, the MP/SOFT methodology provides a quantitative description of both the initial classical dephasing dynamics and the later quantum coherent recurrencies as well as the effect of temperature on the classical and quantum relaxation time scales. The efficiency of the MP/SOFT method is demonstrated in terms of the moderate number of coherent states, required by the expansion introduced by Eq. (10), with $n=100$ for $\hbar\omega\beta=\sqrt{2}$ and $n=500$ for $\hbar\omega\beta=\sqrt{2}/2$, respectively.

Figures 2 and 3 compare the real and imaginary parts of the position-position correlation functions computed according to Eq. (3), with $A(\mathbf{x}')=\mathbf{x}'$ and $\hat{B}=\hat{\mathbf{x}}$. The MP/SOFT results (solid lines) are compared to benchmark grid-based quantum-mechanical calculations (dots) and classical Boltz-

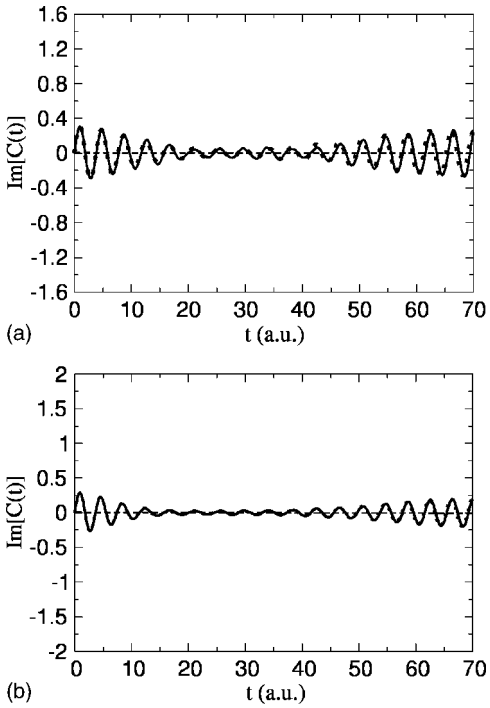

FIG. 3. Comparison of imaginary parts of the position-position correlation functions obtained according to the MP/SOFT method (solid lines), benchmark grid-based SOFT calculations (dots), and the classical Boltzmann ensemble averages (thin-dashed lines) for the asymmetric quartic potential, introduced by Eq. (18). The system is initially prepared at thermal equilibrium on the potential energy surface introduced by Eq. (19) at two different temperatures corresponding to (a) $\hbar\omega\beta=\sqrt{2}$ and (b) $\hbar\omega\beta=\sqrt{2}/2$.

mann ensemble averages (thin-dashed) at two different temperatures corresponding to $\hbar\omega\beta=\sqrt{2}$ and $\hbar\omega\beta=\sqrt{2}/2$ in panels (a) and (b), respectively.

Figures 2 and 3 show that the MP/SOFT methodology provides an accurate and efficient description of both the real and imaginary parts of thermal correlation functions $C(t)$, as influenced by both classical- and quantum-dynamical effects at different temperatures. In correspondence to Fig. 1, it is shown that the MP/SOFT approach provides an exact description of dephasing and rephasing dynamics as determined by the coherent wave packet motion on the highly anharmonicity quartic potential.

The results presented in this paper are not surprising since the generalization of the MP/SOFT method to computations of thermal correlation function, introduced in Sec. II is both formally and numerically exact. The comparisons to benchmark calculations, however, demonstrate at least the potentiality of the MP/SOFT approach for numerically accurate and efficient calculations of finite-temperature expectation values and thermal-correlation functions in systems with significant quantum-mechanical behavior. Note that the MP/SOFT method does not suffer from the "sign problem" that usually defy the capabilities of real-time path-integral Monte Carlo methods[57] and is able to properly describe quantum-mechanical phenomena that might defy the capabilities of approximate semiclassical approaches.

IV. CONCLUDING REMARKS

We have shown how to generalize the MP/SOFT method to rigorous computations of thermal-equilibrium density matrices, finite-temperature time-dependent expectation values, and thermal correlation functions. The method involves the imaginary-time integration of the Bloch equation and the evaluation of Heisenberg time-evolution operators through real-time propagation in dynamically adaptive coherent-state representations. The generalized MP/SOFT methodology, which is common to both real- and imaginary-time propagation, relies on the recursive application of the time evolution operator, as defined by the Trotter expansion to second-order accuracy, in nonorthogonal and dynamically adaptive coherent-state representations generated according to the matching-pursuit algorithm.

We have demonstrated the accuracy and efficiency of the generalized MP/SOFT approach for computations of thermal correlation functions, as compared to benchmark quantum-mechanical calculations for a model system in reduced dimensionality. The reported results show that the MP/SOFT methodology provides a quantitative description of both classical dephasing dynamics and quantum coherent recurrencies as well as the effect of temperature on the classical and quantum relaxation time scales. While the study has been focused only on a reduced dimensional model system that allowed for rigorous comparisons with classical, semiclassical, and benchmark quantum calculations, the results reported in this paper at least demonstrate the potentiality of the MP/SOFT method as applied to the description of thermal correlation functions of complex (i.e., nonintegrable) quantum systems. Work in progress in our research group involves the application of the general computational approach introduced in this paper to studies of thermal correlation functions in multidimensional model systems.

ACKNOWLEDGMENTS

V.S.B. acknowledges supercomputer time from the National Energy Research Scientific Computing Center and financial support from a Research Innovation Award No. RI0702 from Research Corporation, a Petroleum Research Fund Award No. PRF 37789-G6 from the American Chemical Society, a junior faculty award from the F. Warren Hellman Family, a National Science Foundation (NSF) Career Program Award No. CHE-0345984, the NSF Nanoscale Exploratory Research (NER) Award No. ECS-0404191, and start-up package funds from the Provost's Office at Yale University.

[1] Y. Wu and V. Batista, J. Chem. Phys. **118**, 6720 (2003).
[2] Y. Wu and V. Batista, J. Chem. Phys. **119**, 7606 (2003).
[3] Y. Wu and V. Batista, J. Chem. Phys. **121**, 1676 (2004).
[4] D. Neuhauser, J. Chem. Phys. **100**, 9272 (1994).
[5] W. Zhu, J. Zhang, and D. Zhang, Chem. Phys. Lett. **292**, 46 (1998).
[6] G. Schatz, M. Fitzcharles, and L. Harding, Faraday Discuss. Chem. Soc. **84**, 359 (1987).
[7] D. Clary, J. Phys. Chem. **98**, 10678 (1994).
[8] R. Kosloff, Annu. Rev. Phys. Chem. **45**, 145 (1994).
[9] J. Fair, D. Schaefer, R. Kosloff, and D. Nesbitt, J. Chem. Phys. **116**, 1406 (2002).
[10] J. Echave and D. Clary, J. Chem. Phys. **100**, 402 (1994).
[11] H. Yu and J. Muckerman, J. Chem. Phys. **117**, 11139 (2002).
[12] M. Hernandez and D. Clary, J. Chem. Phys. **101**, 2779 (1994).
[13] D. Charlo and D. Clary, J. Chem. Phys. **117**, 1660 (2002).
[14] J. Bowman, J. Phys. Chem. A **102**, 3006 (1998).
[15] D. Xie, R. Chen, and H. Guo, J. Chem. Phys. **112**, 5263 (2000).

[16]S. Anderson, T. Park, and D. Neuhauser, Phys. Chem. Chem. Phys. **1**, 1343 (1999).
[17]M. D. Feit, J. A. Fleck, Jr., and A. Steiger, J. Comput. Phys. **47**, 412 (1982).
[18]M. D. Feit and J. A. Fleck, Jr., J. Chem. Phys. **78**, 301 (1983).
[19]D. Kosloff and R. Kosloff, J. Comput. Phys. **52**, 35 (1983).
[20]H. Tal-Ezer and R. Kosloff, J. Chem. Phys. **81**, 3967 (1984).
[21]T. Park and J. Light, J. Chem. Phys. **85**, 5870 (1986).
[22]N. Makri and W. Miller, J. Chem. Phys. **116**, 9207 (2002).
[23]E. Jezek and N. Makri, J. Phys. Chem. A **105**, 2851 (2001).
[24]A. Nakayama and N. Makri, J. Chem. Phys. **119**, 8592 (2003).
[25]J. Poulsen, G. Nyman, and P. Rossky, J. Chem. Phys. **119**, 12179 (2003).
[26]C. Lawrence, A. Nakayama, N. Makri, and J. Skinner, J. Chem. Phys. **120**, 6621 (2004).
[27]D. Reichman, P. Roy, and G. Voth, J. Chem. Phys. **113**, 919 (2000).
[28]Q. Shi and E. Geva, J. Chem. Phys. **119**, 9030 (2003).
[29]Y. Yonetani and K. Kinugawa, J. Chem. Phys. **119**, 9651 (2003).
[30]M. Jarrell and J. Gubernatis, Phys. Rep. **269**, 133 (1996).
[31]A. Horikoshi and K. Kinugawa, J. Chem. Phys. **119**, 4629 (2003).
[32]E. Rabani and D. Reichman, J. Chem. Phys. **116**, 6271 (2002).
[33]D. Reichman and E. Rabani, Phys. Rev. Lett. **87**, 265702 (2001).
[34]S. Mallat and Z. Zhang, IEEE Trans. Signal Process. **41**, 3397 (1993).
[35]E. Heller, Chem. Phys. Lett. **34**, 321 (1975).
[36]M. J. Davis and E. J. Heller, J. Chem. Phys. **71**, 3383 (1979).
[37]E. Heller, J. Chem. Phys. **75**, 2923 (1981).
[38]R. Coalson and M. Karplus, Chem. Phys. Lett. **90**, 301 (1982).
[39]S. Sawada, R. Heather, B. Jackson, and H. Metiu, Chem. Phys. Lett. **83**, 3009 (1985).
[40]K. G. Kay, J. Chem. Phys. **91**, 107 (1989).
[41]M. Ben-Nun and T. Martinez, J. Chem. Phys. **108**, 7244 (1998).
[42]K. Thompson and T. Martinez, J. Chem. Phys. **110**, 1376 (1999).
[43]M. Ben-Nun and T. Martinez, Adv. Chem. Phys. **121**, 439 (2002).
[44]D. V. Shalashilin and B. Jackson, Chem. Phys. Lett. **291**, 143 (1998).
[45]L. Andersson, J. Chem. Phys. **115**, 1158 (2001).
[46]D. Shalashilin and M. Child, J. Chem. Phys. **113**, 10028 (2000).
[47]D. Shalashilin and M. Child, J. Chem. Phys. **115**, 5367 (2001).
[48]M. Beck, A. Jackle, G. Worth, and H. Meyer, Phys. Rep. **324**, 1 (2000).
[49]M. Nest and H. Meyer, J. Chem. Phys. **119**, 24 (2003).
[50]Y. Wu and V. Batista, J. Chem. Phys. (in press).
[51]R. Feynman, in *Statistical Mechanics* (Benjamin, Reading, 1972).
[52]W. H. Press, B. P. Flannery, S. A. Teukolsky, and W. T. Vetterling, in *Numerical Recipes* (Cambridge University Press, Cambridge, 1986), Chap. 12.
[53]V. Guallar, V. Batista, and W. Miller, J. Chem. Phys. **113**, 9510 (2000).
[54]V. Guallar, V. Batista, and W. Miller, J. Chem. Phys. **110**, 9922 (1999).
[55]M. Petkovic and O. Kuhn, J. Phys. Chem. A **107**, 8458 (2003).
[56]J. Shao and N. Makri, J. Phys. Chem. A **103**, 7753 (1999).
[57]S. Caratzoulas and P. Pechukas, J. Chem. Phys. **104**, 6265 (1996).